Journal of ELECTRONIC MATERIALS, Vol. 38, No. 7, 2009
DOI: 10.1007/s11664-009-0725-3

Special Issue Paper

Efficient Switched Thermoelectric Refrigerators for Cold Storage Applications

U. GHOSHAL[1,2] and A. GUHA[1]

1.—Sheetak Inc., Austin, TX 78746, USA. 2.—e-mail: ghoshal@sheetak.com

We present switching methods that make thermoelectric refrigerators efficient and optimal for all cold storage applications. These temporal methods double the coefficient of performance (COPs) of the refrigerators during cooling transients and allow highly energy-efficient operation in the steady state by turning off the thermoelectric devices both electrically and thermally so as to avoid back-conduction of heat through the devices. We describe thermoelectric refrigerator cooling engines that attain these enhancements without using any unreliable mechanically moving switching components such as pumps. These switching techniques can provide a fivefold reduction in energy consumption of cold storage refrigerators.

Key words: Thermoelectric, switched, efficient, COP, refrigerators, cold storage, nonmoving, thermal diode, thermal capacitor, PCM, phase change materials

INTRODUCTION

Solid-state thermoelectric coolers could potentially revolutionize refrigeration systems if the coefficient of performance (COP) of coolers could be tripled to match that of mechanical vapor compression refrigerators, and if the cost of the system could be scaled down significantly. Most efforts over the last decade have focused on novel materials systems promising materials with a higher figure of merit. Unfortunately, in spite of materials advances such as the reduction of thermal conductivity in superlattice planes,[1] transport and confinement in nanowires and quantum dots,[2] and optimization of ternary and quaternary chalcogenides,[3] practical advances in realizing functional coolers have been minimal. The best results of functional couples based on nanostructured bismuth telluride bulk materials[4] indicate a maximum figure of merit of 1.2 at room temperature—an important advance for attaining a COP $\approx$ 1.0 for ΔT = 30 K. However, the performance still falls far short of being competitive with vapor compression refrigeration cycles.

The other practical advance at the system level during the last decade has been the use of counterflow fluid heat exchangers for air-conditioning applications. Although the advantages of the "spatial" counterflow heat exchangers in cooling fluids were known several decades ago,[5] it was recently championed by BSST, and several air/fluid conditioning systems have been realized in practice. The effective COPs can be increased by a factor of 1.5 to 2.0 by reducing the temperature differential across the coolers and properly optimizing the currents of the spatial stages. Unfortunately, as pointed out by Bell,[6] the COP advantages are lost when steady-state temperatures are attained. Furthermore, the spatial method often necessitates the use of unreliable and costly mechanical pumps if liquid cooling/heat rejection loops are used.

In cold storage applications, especially in the ubiquitous low-cost freezers, water dispensers, and compact refrigerators, it is very important to thermally isolate the cold chamber in the steady state from the ambient. This thermal isolation is essential for conserving electrical power. Typically, the refrigerator designer incorporates the best heat rejection sinks and fans in order to alleviate the hot-side temperature of the inefficient thermoelectric coolers, subject to cost constraints. Although the design may meet the specifications in the active cooling cycle, the same low-conduction heat rejection

(Received July 29, 2008; accepted February 9, 2009; published online March 4, 2009)

path becomes a leakage conduit when the thermoelectric coolers are turned off. This problem prevents the coolers from being deactivated under steady-state conditions. Hence the energy efficiency ratings of thermoelectric refrigerators are significantly lower than those of vapor compressor refrigerators. Currently, there is no commercially available thermoelectric refrigerator that has an on/off refrigeration cycle, and none qualify for standardized efficiency ratings.

In this paper, we describe novel switched thermoelectric coolers that solve the above problems and result in high-efficiency cold storage units. The switching methods outlined are described in the time domain, although both spatial and temporal implementations are possible. These implementations are very different from the early switched thermoelectric coolers[7,8] by Ghoshal wherein the primary focus was increasing the temperature differential in transient operation. It is also different from the research described by Omer et al.[9] in that the timing of the steady-state switching events, the configurations, and the components described here are more optimal for high energy efficiency.

COEFFICIENT OF PERFORMANCE (COP) FOR THE FIRST TRANSIENT

The interval during which the cold chamber cools from ambient to a lower temperature set-point close to 0°C is called the first transient. The analysis presented in this section shows that it is important for the thermoelectric devices to be turned off at an optimal time to maximize the COP for the first transient. The first transient determines the time interval needed to cool the objects in the cold chamber at the start and also sets the heat rejection capacity of the external heat sinks.

Figure 1 shows a schematic diagram of an idealized refrigerator cooled by a thermoelectric cooler. The hot side is clamped at the ambient temperature T_0 (an assumption that will be justified in the "Thermal Switching Components" section) and the cold side/chamber is cooled from the ambient T_0 to a temperature $T_C(t)$ that is a function of time.

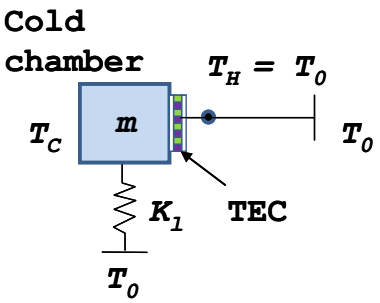

Fig. 1. Schematic of the TEC-cooled refrigerator for analysis of the first transient.

Let

S: Effective Seebeck coefficient of the TEC module
R: Electrical resistance of the TEC module
K: Thermal conductance of the TEC module
$T_C'(t)$: Temporal moving average of $T_C(t)$
$T_{C\infty}$: Steady-state temperature of the cold chamber
$\Delta T(t)$: Temperature differential across the TEC
$\Delta T'(t)$: Temporal moving average of ΔT
$\Delta T_{C\infty}$: Steady-state value of ΔT
m: Mass of the objects/materials in the cold chamber
C: Effective specific heat capacity of the mass m
I: Electric current biasing the TEC
Q: Cooling power of the TEC
K_l: Leakage thermal conductance from ambient to the cold chamber

The cooling power Q at the cold end is given by the relation:

$$\begin{aligned} Q &= SIT_C - \frac{1}{2}I^2R - K(T_0 - T_C) \\ &= -mC\frac{dT_C}{dt} + K_l(T_0 - T_C). \end{aligned} \tag{1}$$

Rearranging the terms,

$$\frac{dT_C}{dt} = -\frac{(T_C - T_{C\infty})}{\tau}, \tag{2}$$

where

$$T_{C\infty} = \frac{(K + K_l)T_0 + \frac{1}{2}I^2R}{K + K_l + SI}$$

and

$$\tau = \frac{mC}{K + K_l + SI}. \tag{3}$$

For a current step of magnitude I, Eq. 2 can be solved to yield $T_C(t)$:

$$T_C(t) = T_{C\infty} - (T_{C\infty} - T_0)\,e^{-t/\tau}. \tag{4}$$

The coefficient of performance $\eta(t)$ of the refrigerator at any instant t in the transient case is given by the ratio of the cumulative cooling power to the total energy expended by the source.

$$\eta(t) = \frac{\int_0^t Q\,dt}{\int_0^t P\,dt} = \frac{\int_0^t \left[SIT_C - \frac{1}{2}I^2R - K(T_0 - T_C)\right]\,dt}{\int_0^t \left[SI(T_0 - T_C) + I^2R\right]\,dt}. \tag{5}$$

For $t > 0$, $I(t)$ is constant, and Eq. 5 can be simplified to

$$\begin{aligned} \eta(t) &= \frac{SI\int_0^t T_C dt - \frac{1}{2}I^2Rt - K\left(T_0 t - \int_0^t T_C dt\right)}{SI\left(T_0 t - \int_0^t T_C dt\right) + I^2Rt} \\ &= \frac{SIT_C' - \frac{1}{2}I^2R - K(T_0 - T_C')}{SI(T_0 - T_C') + I^2R}, \end{aligned} \tag{6}$$

where $T'_C = \frac{\int_0^t T_C\,dt}{t}$ is the time-moving average of the cold-end temperature. The expression in Eq. 6 is similar to the standard expression for COP with the cold-end temperature held constant. The only difference is that the term T_C is replaced by its moving average T'_C.

Substituting the expression for T_C from Eq. 4, we get

$$T'_C = T_{C\infty} - (T_{C\infty} - T_0)\left(\frac{1 - e^{-t/\tau}}{t/\tau}\right). \quad (7)$$

If we define $\Delta T_{C\infty} = T_0 - T_{C\infty}$, we get the following simplified expressions for the temperature differential ΔT and its time-moving average $\Delta T'$:

$$\Delta T = \Delta T_{C\infty}\left(1 - e^{-t/\tau}\right),$$

$$\Delta T' = \Delta T_{C\infty}\left[1 - \frac{\left(1 - e^{-t/\tau}\right)}{t/\tau}\right]. \quad (8)$$

Figure 2 shows the plots of the temperature differentials ΔT and $\Delta T'$ normalized by their steady-state value ($\Delta T_{C\infty}$) and the ratio of $\Delta T'/\Delta T$, as a function of t/τ. It is interesting to note that $\Delta T' < \Delta T$ for all times and $\Delta T'/\Delta T \to 1$ only under steady-state conditions ($t/\tau \to \infty$). This implies that the COP during the transient is always greater than the COP of the thermoelectric cooler with the same temperature differential under steady-state conditions. In fact, at short intervals of time ($t/\tau \to 0$) and very small temperature differentials, $\Delta T'/\Delta T \to 0.5$ and the COP under transient conditions is twice that of the steady-state condition. For reasonable temperature differentials, the better condition is approximately when $t/\tau = 2$, $\Delta T'/\Delta T = 0.66$ and $\Delta T/\Delta T_{C\infty} = 0.87$.

The COP enhancement in transients is equivalent to COP advantages in counterflow heat exchangers in spatial coolers.[5,6] In fact, there is a general equivalence in the temporal and spatial equations, if we realize that the derivative $mC\,dT_C/dt$ in the time domain is replaced by $\dot{m}C\,dT_C/dx$ in the spatial domain. However, each implementation has its specific design characteristics.

In the case when the current $I(t)$ is not constant and has a time-domain profile, numerical methods are the best in evaluating the COPs. The most popular constraint in refrigeration is the proportional excitation, i.e., $I(t) \propto \Delta T$, for which the COP advantages are somewhat better than that of the constant-current case and can double the COP over a larger time interval.

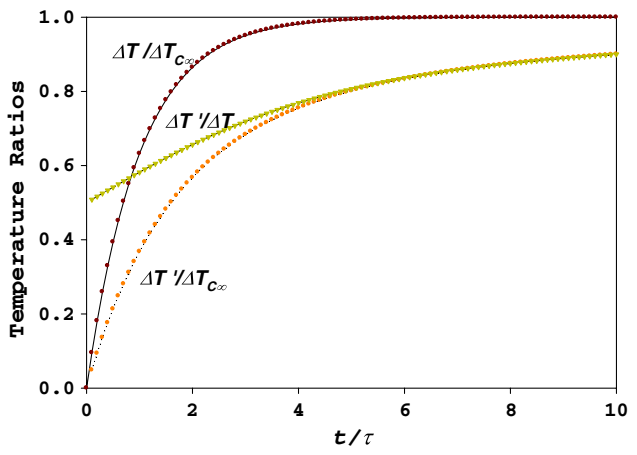

Fig. 2. Temporal variation of the ratios $\Delta T/\Delta T_{C\infty}$, $\Delta T'/\Delta T_{C\infty}$, and $\Delta T'/\Delta T$.

THERMAL SWITCHING COMPONENTS

We use thermal capacitors filled with water or phase-change materials (PCMs) at the heat sinks to clamp the hot-side temperature of the refrigerator during the transients. PCM capacitors are designed such that the heat flow is distributed throughout its volume without incurring large temperature drops in the capacitor, i.e., the capacitors have conductor structures with large Biot number. We have utilized thermal capacitors to clamp the hot end of a thermoelectric cooler at temperatures ~30°C. The use of thermal capacitors at the hot end can reduce the total temperature differentials during transients by a factor of two, and thereby result in higher COPs during the active transients. The thermal capacitors are placed in parallel with the heat rejection path so that there are no additional temperature losses.

In order to reduce the power consumption of the refrigerator after the first transient and in the steady state, the thermoelectric cooler is turned off and activated intermittently to compensate for the heat leakage during the off state and maintain the cold chamber temperature within specified limits. The leakage is determined by the thermal conduction across the refrigerator walls and by the thermal conduction through the TECs. The cooling engine is designed such that the leakage is dominated by the thermal conduction through the TECs. The design allows faster cooling but necessitates the use of a thermal diode to stop the back-conduction through

Table I. Classification of Thermal Diodes

Method	Moving?	Diodicity	Type
Fan	Yes	~3	Active
Water pumped loops	Yes	~10	Active
Air diaphragms	Yes	~10	Active
Shape-memory switches	Yes	~10	Passive
Solid-state rectifiers[10]	No	~0.1	Passive
Radiative diodes	No	~5	Passive
Tesla fluid valve[11]	No	~3	Passive
Thermosyphons	No	~5	Passive
Vapor Diodes™ (proprietary)	No	>150	Passive

the TECs. Table I shows the different methods of fabricating the thermal diode. The diodicity γ is the ratio of the thermal conductance in the forward conducting direction to that in the reverse blocking direction. The thermal diodes investigated in our research and our prototypes have $\gamma \geq 120$.

SWITCHING CYCLES

Figure 3 shows the schematic of a typical thermoelectric refrigerator that rejects heat via an external thermal conductance K_h to the ambient at temperature T_0. The thermal conductance K_h may represent the conductance of a heat sink and fan assembly or that of a liquid cooling loop. The temperature difference between the hot end of the thermoelectric cooler and the ambient in this traditional configuration can be estimated by the following relation:

$$\Delta T_{Ext} = T_H - T_0 = \frac{Q}{K_h}\left(1 + \frac{1}{\eta(\Delta T_{TEC})}\right), \qquad (9)$$

where $\eta(\Delta T_{TEC})$ is the COP of the thermoelectric cooler at a given bias current and a temperature differential ΔT_{TEC}, as shown in Fig. 4. Usually $\eta(\Delta T_{TEC}) \ll 1$, and ΔT_{Ext} is large, of the order of 20 K and $\Delta T_{TEC} \approx 45$ K. If the thermoelectric cooler is turned off, heat flows back from the hot heat rejection unit through the thermoelectric cooler, and as leakage through the chamber walls. This backflow of heat quickly warms the cold chamber to the ambient temperature. If the thermal conductance of the thermoelectric cooler (K) and that of the heat rejection unit (K_h) are reduced so as to slow down the warming process, the cooling performance in the active mode becomes poor. Hence the thermoelectric cooler needs to remain activated to maintain the cold temperature. The energy consumption of traditional thermoelectric refrigerators is very high and not competitive with alternative technologies.

The simple switched thermoelectric cooler configuration shown in Fig. 5 can solve the cold storage problems using the highly energy-efficient steady-state cycle shown in Fig. 6. In this configuration, a diode is inserted in series with the external heat conductance, and a thermal capacitor is introduced in parallel with the heat rejection path. We assume the forward conductance of the thermal diode $K_{DF} = \sqrt{\gamma}K \gg K$ and the reverse conductance $K_{DR} = K/\sqrt{\gamma} \ll K$. During the active (ON) portion of the cycle, the thermoelectric refrigerators cools the cold chamber from the upper-limit T_{SU} of the set-point temperature (T_S) to its lower limit T_{SL}. The time duration of the on portion of the cycle can be estimated from Eq. 2:

$$\tau_{on} = \tau \frac{\Delta T_S}{(T_S - T_{C\infty})} = \frac{mC}{K + K_l + SI} \cdot \frac{\Delta T_S}{(T_S - T_{C\infty})}, \qquad (10)$$

where $\Delta T_S = T_{SU} - T_{SL}$. In contrast with the traditional thermoelectric refrigerator discussed above, when the thermoelectric cooler is deactivated in the off portion of the cycle, the thermal diode completely isolates the cooler and the cold chamber from the heat rejection unit. The chamber can warm up by heat leaking through the insulation in the chamber

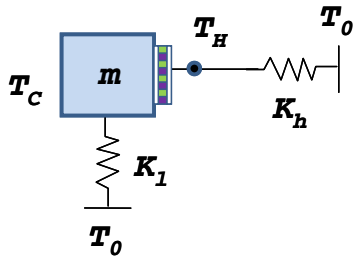

Fig. 3. Schematic of a conventional thermoelectric refrigerator with an effective heat rejection conductance K_h to the ambient.

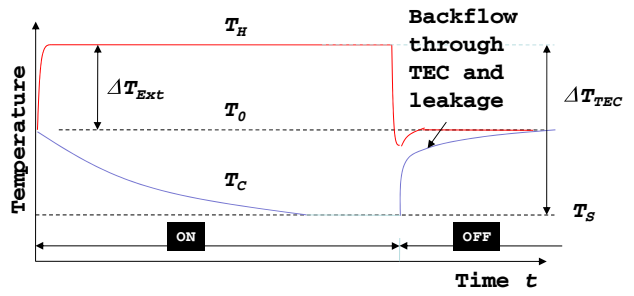

Fig. 4. Graph of typical cooling characteristics of the conventional thermoelectric refrigerator shown in Fig. 3.

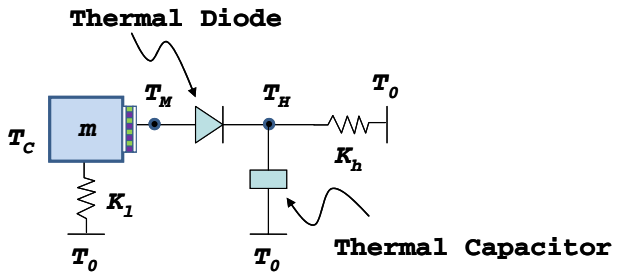

Fig. 5. Schematic of the simplest switched thermoelectric cooler configuration.

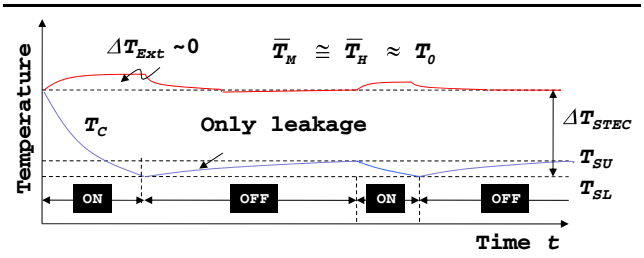

Fig. 6. Graph of typical cooling characteristics of the switched thermoelectric cooler shown in Fig. 5.

walls. The time duration for the temperature rise from T_{SL} to T_{SU} during the off portion can be approximated by an exponential response:

$$\tau_{off} = \frac{mC}{K_l} \cdot \frac{\Delta T_S}{(T_0 - T_S)}. \quad (11)$$

The duty cycle D of the activation of the thermoelectric cooler is simply

$$D = \frac{\tau_{on}}{\tau_{on} + \tau_{off}},$$

i.e.,

$$D = \frac{1}{1 + \frac{(K+K_l+SI)}{K_l} \cdot \left[\frac{T_S - T_{C\infty}}{T_0 - T_S}\right]}. \quad (12)$$

If the bias current is normalized by the maximum device current I_{max}, i.e., $I = xI_{max} = xST_S/R$,

$$D = \frac{1}{1 + \left[1 + (1 + xZT_S)\frac{K}{K_l}\right] \cdot \left[\frac{T_S - T_{C\infty}}{T_0 - T_S}\right]}, \quad (13)$$

where $Z = S^2/(KR)$ is the figure of merit of the thermoelectric device. For typical compact refrigerator applications with T_S = 275 K, $T_{C\infty}$ = 260 K, T_0 = 300 K, x = 0.6, K = 2 W/K, ZT_S = 1, and K_l = 0.3 W/K, D = 0.12. The thermoelectric cooler can be turned on for only 12% of its cycle during the steady state to maintain the temperature of the cold chamber at T_S.

The heat capacity of the thermal capacitor is large enough to hold the temperature T_M and T_H to their (cycle) mean values, $\bar{T}_M$ and $\bar{T}_H$ during the 'on' transients.

$$\bar{T}_M = \bar{T}_H = T_0 + D\frac{Q}{K_h}\left(1 + \frac{1}{\eta(\Delta T_{STEC})}\right) \approx T_0,$$

$$\Delta T_{Ext} = D\frac{Q}{K_h}\left(1 + \frac{1}{\eta(\Delta T_{STEC})}\right) \rightarrow 0.$$

The mean temperature differential across the switched thermoelectric cooler $\Delta T_{STEC} = (T_0 - T_S) \approx$ 25 K is thus substantially lower than the corresponding temperature differential in the traditional thermoelectric refrigerator ($\Delta T_{TEC} \approx$ 45 K). Hence, the COP of the switched thermoelectric cooler is much higher during the on cycle. This effect further increases the energy efficiency by another factor of two than that predicted by simple duty-cycle enhancements.

The total power dissipation per cycle P can be estimated from the equation

$$P(I) = D(S\Delta T_{STEC} + IR)I = \frac{[S(T_0 - T_S) + IR]I}{1 + \frac{(K+K_l+SI)}{K_l} \cdot \left[\frac{T_S - T_{C\infty}(I)}{T_0 - T_S}\right]}, \quad (14)$$

where $T_{C\infty}(I)$ is given by Eq. 3. The function $P(I)$ can be minimized for determining the optimal bias current I for a given set of parameters. Interestingly, the optimal current I_{OPT} for the simple switched thermoelectric cooler configurations shown in Fig. 5 is the same as the standard expression for maximum COP in the usual theory,

$$I_{OPT} = \frac{Z(T_0 - T_S)}{R\left(\sqrt{1 + 0.5Z(T_0 + T_S)} - 1\right)}. \quad (15)$$

The minimum power dissipation is approximately three to five times lower than configurations without switching elements. Note that the switched thermoelectric coolers make the performance independent of the heat rejection conductance K_h and can be exploited to build lower-cost systems. More detailed theory about power optimization in related switched thermoelectric cooler configurations is beyond the scope of this paper, and will be presented elsewhere.

MEASUREMENTS

We have incorporated the thermal diode and thermal capacitors in a variety of switched thermoelectric cooling engines and have verified the switching cycles. One such early test prototype with a configuration corresponding to Fig. 5 is discussed in this section.

The test setup comprised of a copper block cooled with a generic thermoelectric cooler module (TEC 12706) and a vapor diode ($\gamma \approx 120$) attached to the hot side of the cooler module. The TEC was powered with a DC source supplying 7 V and 3 A. The upper and lower set temperature limits (T_{SU} and T_{SL}) were 0°C and 10°C, respectively. The TEC module had K = 0.7 W/K—a value that was verified by independent Q-meters, $I_{max} \approx$ 6 A and $\Delta T_{STEC} \approx$ 30 K. The copper block was insulated with layers of Styrofoam such that the total heat leakage conductance when the TEC module was turned off was K_l = 0.1 W/K. Substituting T_S = 278 K, $T_{C\infty}$ = 268 K, T_0 = 305 K, x = 0.5, and ZT_S = 0.7 in Eq. 13, D = 0.2.

From the measured switching cycle shown in Fig. 7, we obtain a value of D = 0.22 that agrees very well with the theoretical estimate. The same engine and a similar cycle operated in a small water chamber would maintain a steady-state temperature of 5°C while reducing the energy consumption by fivefold when compared with traditional thermoelectric water coolers.

Although the cooling engine performance verifies the theory of switched thermoelectric refrigerators, there are several parasitics and parameters that need to be optimized in a practical refrigerator. One such critical parasitic is the "shuttle" heat capacity of the node labeled T_M that is cycled from ambient (~33°C) to a low temperature ~11°C. Recent designs that capitalize on the shuttle mass will be discussed in future publications.

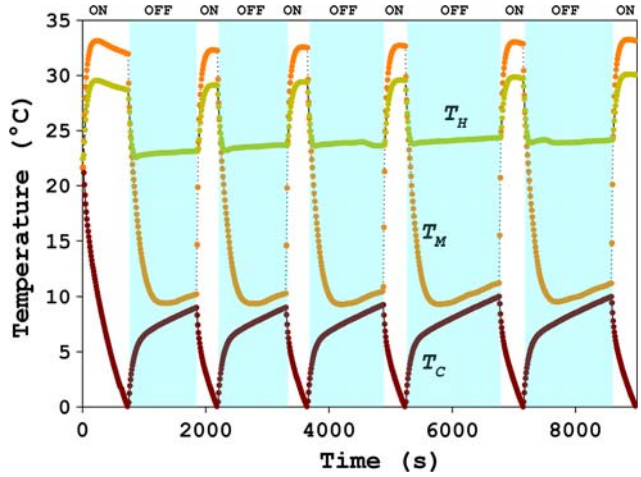

Fig. 7. Measured switching cycle of an experimental water cooling engine. The cold-end sink temperature is denoted by T_C and the temperature of the external heat sink is T_H. T_M labels the "shuttle" node temperature that also represents the hot side of the thermoelectric cooler. The thermoelectric cooler is turned on during a small fraction of the cycle, i.e., the duty cycle is 0.22, and results in a reduction in energy consumption by 4.5 times. The time duration for the last off and on periods were 1430 s and 400 s, respectively.

CONCLUSIONS

We have presented the theory of novel switched thermoelectric coolers exploiting thermal diodes and thermal capacitors, and have experimentally verified the operation of cooling engines in simple configurations. The switching operations double the cooling efficiency during the first transient and results in significant (three- to fivefold) energy savings in cold storage units during the steady state. These system-level enhancements are complementary to advantages of the high-ZT thermoelectric materials technologies. The performance of switched thermoelectric refrigerators is competitive with small mechanical vapor compressor refrigerators, and provides an alternative low-cost, silent, reliable, and ecofriendly refrigeration solution.

ACKNOWLEDGEMENTS

The authors would like to thank other members of the Sheetak team for the success of the switched thermoelectric refrigerators. In particular, we would like to thank James Borak, who was responsible for the machining, fabrication, and measurement of several components of the refrigerator described in this paper.

REFERENCES

1. R. Venkatasubramanian, E. Siivola, T. Colpitts, and B. O'Quinn, *Nature* 413, 597 (2001). doi:10.1038/35098012.
2. T.C. Harman, P.J. Taylor, M.P. Walsh, and B.E. LaForge, *Science* 297, 2229 (2002). doi:10.1126/science.1072886.
3. K.F. Hsu, S. Loo, F. Guo, W. Chen, J.S. Dyck, C. Uher, T. Hogan, E.K. Polychroniadis, and M.G. Kanatzidis, *Science* 303, 818 (2004). doi:10.1126/science.1092963.
4. B. Poudel, Q. Hao, Y. Ma, Y. Lan, A. Minnich, B. Yu, X. Yan, D. Wang, A. Muto, D. Vashaee, X. Chen, J. Liu, M. Dresselhaus, G. Chen, and Z. Ren, *Science* 320, 634 (2008). doi:10.1126/science.1156446.
5. J. Fenton, J. Lee, and R. Buist, U.S. patent 4,065,936 (1978).
6. L. Bell, *Proc. 21st Int. Conf. Thermoelectrics* (2002), p. 477.
7. C. Hilbert, R. Nelson, J. Reed, B. Lunceford, A. Sommader, K. Hu, and U. Ghoshal, *Proc. 18th Int. Conf. Thermoelectrics* (1999), p. 117.
8. A. Miner, A. Majumdar, and U. Ghoshal, *Proc. 18th Int. Conf. Thermoelectrics* (1999), p. 27.
9. S. Omer, S. Riffat, and X. Ma, *Appl. Thermal Engg.* 21, 1265 (2001). doi:10.1016/S1359-4311(01)00010-2.
10. C.W. Chang, D. Okawa, A. Majumdar, and A. Zettl, *Science* 314, 1121 (2006). doi:10.1126/science.1132898.
11. N. Tesla, U.S. patent 1329559 (1920).